

Characterization of *nurf-1* mutation in suppressing of *top-2-induced* embryonic lethality in *C. elegans*

by

Jiaying Bi

A thesis submitted to the Faculty of the University of Delaware in partial fulfillment of the requirements for the degree of Bachelor of Science in Biological Science Major with Distinction

Spring 2022

© 2022 Jiaying Bi
All Rights Reserved

Characterization of *nurf-1* mutation in suppressing of *top-2-induced* embryonic lethality in *C. elegans*

by

Jiaying Bi

Approved: _____
Aimee, Jaramillo-Lambert, Ph.D.
Professor in charge of thesis on behalf of the Advisory Committee

Approved: _____
Jessica, Tanis, Ph.D.
Committee member from the Department of Biological Science

Approved: _____
Carlton Cooper, Ph.D.
Committee member from the Board of Senior Thesis Readers

Approved: _____
Dana Veron, Ph.D.
Chair of the University Committee on Student and Faculty Honors

ACKNOWLEDGMENTS

I would like to acknowledge my PI, Dr. Aimee Jaramillo-Lambert, for allowing me to participate in your lab and complete my senior thesis. I really appreciate this priceless opportunity. I have learned so much by working in your lab for the past year: I was able to acquire and build knowledge in genetics and different scientific techniques. This hands-on experience further fueled my passion for continuing my research career in science and medicine. I would like to thank Dr. Aimee for your incredible patience and for providing honest feedback. I could not imagine conducting my own research and writing a senior thesis until I started working in your lab. You helped to make my dreams come true.

I would also like to thank all of my fellow researchers, Christine, Kent, Nirajan, Lacole, Nancy, Chris, Shannon, and others in lab for your generous help, patience, and kindness. I am very fortunate to have been able to learn and work with all of you.

This manuscript is dedicated to my husband, Luke. Thank you so much for your love and support through all these years. I am never alone on the path to chasing my dream because you will always be my side.

TABLE OF CONTENTS

LIST OF TABLES	vii
LIST OF FIGURES	viii
ABSTRACT	xi
1 INTRODUCTION.....	1
1.1 What is NURF-1 in <i>C. elegans</i> ?	1
1.1.1 Meiosis	1
1.1.2 Role of type II DNA Topoisomerases in meiosis	3
1.1.3 Why do we study <i>nurf-1</i> ?	6
1.1.4 Possible role of NURF-1 in meiosis	9
1.2 <i>C. elegans</i> as model organisms.....	11
1.3 Research Goal.....	13
2 MATERIALS AND METHODS	16
2.1 Strains	16
2.2 Embryonic Viability Assay	16
2.3 Whole-mount DAPI Staining	16
2.4 CRISPR/Cas9-Mediated Genome Editing and Screening.....	17
2.5 Creation of the <i>nurf-1; him-8</i> line	20
3 RESULTS.....	26
3.1 Successful recreation of the <i>nurf-1</i> [E1952K] suppressor allele using CRISPR/Cas9 genome editing	26
3.2 <i>nurf-1</i> [E1952K] allele does not cause embryonic lethality	29
3.3 Characterization of the <i>nurf-1(ude34)</i> [E1952K] allele	31
4 DISCUSSION.....	34

4.1 The Co-suppression mechanism of the <i>top-2-induced</i> embryonic lethality from <i>nurf-1</i> and <i>mep-1</i> remains unknown	34
4.2 Further Direction	38
5 CONCLUSION	40
REFERENCES	41

LIST OF TABLES

Table S1. Strains used in this study	25
---	-----------

LIST OF FIGURES

Figure 1. Double-stranded DNA cleavage and ligation catalyzed by topoisomerase II. 5

During cleavage, the active site tyrosine from each subunit covalently links to the 5' terminal phosphate group on the opposite strands four bases apart. Ligation is the reverse of the process and does not change the chemical structure of the DNA strands. Diagram retrieved from Deweese & Osheroff, 2009.

Figure 2. The *nurf-1* locus on chromosome II. 8

(a) 17 isoforms of *nurf-1* gene (F26H11.2); all isoforms are predicted to produce proteins with different functions. Diagram retrieved from wormbase.org. (b) Genomic structures of the isoform studied in this research, *nurf-1 a*. Mutant allele *n4293Δ* is presented as a 724 bp deletion at the splice donor region of exon 1 and it removes all of exon 1. Diagram retrieved from Andersen et al., 2016.

Figure 3. Structural components of NURF complex in *D. melanogaster* (Drosophila) and in *H. sapiens* (Human). 10

Drosophila NURF complex contains the *C. elegans* NURF-1 ortholog NURF301 and ISWI subunits, co-acting NURF38 and NURF55 subunits. Human NURF complex contains the *C. elegans* NURF-1 ortholog BPTF, and co-acting subunits, SNF2L and RBAP46/48. Retrieved from Alkhatib & Landry, 2011.

Figure 4. Possible mechanism of NURF complex in nucleosome regulation. 11

NURF complex depends on ATP to cause a “sliding” effect between two neighboring nucleosomes and then expose the DNA region for replication, transcription, and repair. Retrieved from Hamiche et al., 1999.

Figure 5. CRISPR/Cas9 Genome Editing in *C. elegans*. 19

Injection was done with an injection mix of Cas9 protein, *dpy-10* crRNA, *dpy-10(cn64)* repair oligonucleotide, universal tracrRNA, *nurf-1*-specific crRNA and *nurf-1*-specific repair oligonucleotide. Rollers were picked and allowed to produce embryos in F1 generation before proceeded to make into single worm lysates. Single worm lysates of F1 rollers then went through PCR, enzymatic digest, and finally visualized on agarose gel. In the F2 generation, heterozygous or homozygous non-rollers were

picked, lysed, and processed using the same procedure. Finally, selected F3 worms were sequenced to confirm the induced point mutation. F3 plates were maintained under standard conditions.

Figure 6. Genetic cross procedure to obtain males using *him-8(e1489)* line. 22

(a) Creation of *nurf-1 (n4293Δ); him-8(e1489)* line that produce male progeny. In F2 progeny, *mnC1/mnC1::GFP* has the phenotype of being paralyzed. Hence the only genotype that carrying the GFP phenotype without looking paralyzed was *n4293Δ/mnC1::GFP*. F3 hermaphrodite with GFP were cultured in 40 single worm plates and allowed self-cross. Only plates with male progeny [indicating presence of homozygous *him-8(e1489)*] were maintained. (b) Creation of *nurf-1 (ude34)[E1952K]; him-8(e1489)* line that produce male progeny. (c) To confirm the remaining of the single missense mutation E1952K, whole plate lysis was performed on the F4 progeny, followed by PCR amplification and *MseI* enzymatic digest. The result of digestion was finally visualized through gel electrophoresis

Figure 7. Gel images of the *MseI* enzymatic digest results on F1, F2, and F3 worms after CRISPR/Cas9 genome editing on N2 worms. 27

Non-digested bands and digested bands are shown with arrows. (a) Analysis of 36 F1 rollers. Lanes with complete or partial digestion are circled. (b) Analysis of F2 progeny from the circled F1 rollers (whole plate lysates). F2 progeny from roller 9.6 exhibits possible homozygosity, while progeny from roller 9.24 and roller 5.2 exhibit possible heterozygosity. (c) Analysis of non-roller F2 progeny from the circled F1 rollers (single worm lysates). The circled four worms exhibit possible homozygosity. (d) Analysis of F3 progeny from the circled F2 worms (whole plate lysates). All exhibit possible homozygosity.

Figure 8. DNA sequencing results to confirm the success in CRISPR/Cas9 genome editing. 28

This figure depicts the comparison between the desired sequence (the top line) and the CRISPR/Cas9-edited sequence (the bottom line). The bottom line was derived from the undigested DNA fragment of the F3 progeny from worm 9.6.1. The sequences colored in blue highlight the forward and reverse primers used for PCR amplification; the sequence colored in green highlights the crRNA for E1952K; the sequence colored in pink highlights the *MseI* restriction site [*T[^]TAA*]; the AAA colored in blue next to the pink *TT* shows the site of desired point mutation *E1952K*; letter *Ns* are undetermined nucleotides in the sequencing read.

Figure 9. Average percent embryonic viability in N2 and *nurf-1* mutant hermaphrodites at 20°C. 30

From left to right: N2: WT control line; SD=0.3. *nurf-1(n4293Δ)/mnC1*: heterozygous control line; genotype with one mutant allele carrying a 724bp deletion; non-sterile; SD=0.8; p=0.135. *nurf-1(ude34)* [E1952K]: homozygous CRISPR-recreated line; non-sterile; SD=0.1; p=0.09. *nurf-1(n4293Δ)*: homozygous genotype with a 724 bp deletion on both alleles; sterile; SD=0; p=2.92E-24 (significant to N2 line); p=6.93E-14 (significant to heterozygous control line *nurf-1(n4293Δ)/mnC1*) Error bars on top of the columns indicate standard deviation of at least three independent experiments. The progeny of at least 30 hermaphrodites were scored for each genotype. SD: standard deviation. n: total number of hermaphrodites scored. p: statistical significance, two-tailed distribution, heteroscedastic. ns: not significantly different; p ≥0.05. ****: significantly different; p ≤0.0001.

Figure 10. Characterization of *C. elegans nurf-1* mutations. 32

Whole-mount DAPI staining images. Top: homozygous *nurf-1(n4293Δ)* males and hermaphrodites. No germline defect was observed in males. In hermaphrodites, no defect observed in sperms or oocytes. However, a significant portion of the worms showed defected embryos in the region near the vulva. This indicates a possible defect in fertilization or embryogenesis. Middle: heterozygous *nurf-1(n4293Δ)/mnC1* control males and hermaphrodites. Meiosis proceeds normally in these germlines. Bottom: homozygous *nurf-1(ude34)*[E1952K] males and hermaphrodites. No defect in sperms, oocytes, or embryos observed. More than 30 worms in each genotype were fixed and stained 24 hours after the L4 stage. Scale bar=100 um.

Figure 11. Reproductive systems in *C. elegans* and score of germline defects in adult worms of each genotype in this study. 33

(b) Cartoon drawing of *C. elegans* gonads of WT hermaphrodites and males. Adapted from wormbook.org. (c) Percent of germline defects in adult worms of each genotype. Heterozygous *nurf-1(n4293Δ)/mnC1* males and hermaphrodites were used as the control group for comparison. For each genotype, 30 adult worms were counted. 28/30 of the homozygous *nurf-1(n4293Δ)* hermaphrodites showed defects. For homozygous *nurf-1(n4293Δ)* males, 0/30 showed defects in the germline. For the CRISPR-created homozygous *nurf-1(ude34)* [E1952K] males and hermaphrodites, 0/30 showed observable germline defect.

Figure 12. Models of predicative protein structures of the *nurf-1* encoded protein and the *mep-1* encoded protein. 37

(a) *nurf-1* encoded protein, which is a subunit in the NURF301-like nucleosome-remodeling factor. The CRISPR-induced single missense mutation E1952K is confidently (pLDDT >70) considered to be located on an α helix on a DDT domain (light blue helix marked in light pink and pointed out by a magenta-colored arrow). (b) *mep-1* encoded protein, which is a MOG interacting and ectopic P-granules protein, aka zinc finger protein. The CRISPR-induced single missense mutation G57D is predicted (pLDDT <50) to happen on a disordered region (colored orange; pointed out by a magenta-colored arrow). Both models retrieved and adapted from alphafold. Deep blue color indicates a very high model confidence (pLDDT >90); light blue color indicates a high model confidence (90 > pLDDT > 70); yellow indicates a low model confidence (90 > pLDDT > 70); orange indicates a very low model confidence (pLDDT < 50). pLDDT, per-residue confidence score.

ABSTRACT

The *nurf-1* gene in *Caenorhabditis elegans* is a Nucleosome Remodeling Factor (NURF) subunit that has crucial roles in chromatin remodeling and transcription regulation. *nurf-1* null mutations cause severe defects in germline cells and lead to embryonic lethality. However, a previous study from our lab showed that *nurf-1* with a single missense mutation that changes the glutamate on position 1954 to a lysine [E1954K] was involved in rescuing embryonic lethality induced by a mutation of the topoisomerase II enzyme [*top-2(it7)*]. Here, *top-2(it7)* is a temperature-sensitive allele, which contains a single missense mutation [R828C] that causes severe defects in chromosomal segregation during spermatogenesis. In fact, *nurf-1*[E1954K] was found to suppress the *top-2*-induced embryonic lethality only in conjunction with another mutation in a gene called *mep-1*, which encodes a zinc-finger protein that is a part of chromatin remodeling complex. Bhandari et. al., 2020 found that the suppressing mutation *mep-1(ude14)* is a single missense mutation [G57D]. In order to begin to elucidate the mechanism of this co-suppression, I started this study by characterizing two *nurf-1* mutants, which includes a deletion allele (*n4293*) and through the recreation of the single missense mutation [E1952K] (1954 to 1952 change is due to a different *nurf-1* isoform). The suppressor mutation was recreated in a wild-type background using the CRISPR-Cas9 genome editing technique [*nurf-1(ude34)*]. The percent embryonic viability in each genotype was determined through an embryonic viability assay. In addition, the gonads in both hermaphrodites and

males in each genotype were observed using whole-mount DAPI staining. We confirmed the severe defects and sterility of the homozygous *nurf-1* deletion in hermaphrodites. However, no germ line defects were observed in the *nurf-1(ude34)* [E1952K] hermaphrodites or males. Also, the suppressor allele *nurf-1(ude34)* [E1952K] showed no significant difference in the percent embryonic viability compared to the wild-type control group. These results indicate that this single missense mutation of *nurf-1(ude34)* [E1952K] does not have meiotic phenotype when in isolation. The mechanism of co-suppression of *nurf-1* and *mep-1* on the *top-2*-induced embryonic lethality might be direct or indirect. A combination of the induced single missense mutation of both *nurf-1* and *mep-1* will be analyzed in future studies. Moreover, further structure-function analyses will help elucidate details of the roles of both *nurf-1* and *mep-1* during meiosis as well as their co-suppression mechanism at a molecular level.

Chapter 1

INTRODUCTION

1.1 What is NURF-1 in *C. elegans*?

1.1.1 Meiosis

Meiosis is the cell division process in forming gametes in eukaryotic cells. During meiosis, the genetic materials are divided into four haploid gametes (Hillers, 2015). Different from mitosis, in which the cell undergoes only one round of division, meiosis includes two stages of cell division, namely Meiosis I and Meiosis II. During Meiosis I, homologous pairs are separated, and the chromosome number is reduced by half (Hillers, 2015). This reduction of chromosome number does not happen during mitosis. The process of Meiosis II is similar to the process of mitosis: from anaphase II, sister chromatids are separated and pulled to each end of the cell to form two new daughter cells. The daughter cells in meiosis are haploid, while the daughter cells in mitosis are diploid. In addition, meiosis only happens in germ cells, while mitosis mainly happens in somatic cells (Libretexts, 2022).

Crossing over is another unique and critical event happens in Meiosis I. During crossing over, genetic materials are exchanged between two non-sister chromatids of the paired homologous chromosomes. This event prevents forming two genetically identical daughter cells (Hillers, 2015). Together with independent assortment, crossing over ensures the genetic diversity amongst the gametes (Libretexts, 2022).

Germ cells start the process of Meiosis I by entering Prophase I. During prophase, synapsis of homologous chromosomes takes place as well as the process of crossing over. This happens during the subphase of prophase I, which is called pachytene. Before pachytene, the cell must undergo two subphases, leptotene and zygotene, to be prepared for synapsis. The chromosomes start to condense during leptotene, and their telomeres are attached to the nuclear membrane. Next, synapsis starts during zygotene: a synaptonemal complex is formed between homologous chromosomes. However, this process is not completed until the pachytene stage. During pachytene, exchange of genetic material via crossing over happens between two non-sister chromatids. After pachytene, the cell goes through two other subphases, diplotene and diakinesis: synapsis ends in diplotene as the synaptonemal complex disappears, meanwhile, the homologous pairs are still attached at chiasmata. During diakinesis, the chromosomes are observed to be the most condensed and the cell is getting prepared to enter metaphase I (BioNinja, 2022). The chromosomes are lined up at the metaphase plate during metaphase I. After metaphase I, the cell enters anaphase I, when the aligned chromosome pairs are pulled toward each end of the cell. The final stage in Meiosis I is telophase I, when the chromosomes reach the opposite pole and the cytoplasm divides to form two haploid daughter cells (Libretexts, 2022). The formed daughter cells will enter Meiosis II for the second round of cell division. Meiosis II is analogous to the process of mitosis, it can be divided into subphases of prophase II, metaphase II, anaphase II, telophase II, and cytokinesis. Just as during mitosis, the chromosomes condense during prophase II; sister chromatids are lined up

at the metaphase plate during metaphase II; sister chromatids are pulled toward each end of the cell during anaphase II. During telophase II and cytokinesis, the chromosomes arrive at each end of the cell and decondense, the nuclear envelopes reform, and the cell is divided into two haploid daughter cells. The main differences between Meiosis II and Mitosis are: only one set of chromosomes are lined up and separated during Meiosis II, while there are two sets of homologous chromosomes during mitosis. Also, two haploid daughter cells are formed at the end of Meiosis II, while at the end of mitosis, two diploid daughter cells are formed (Libretexts, 2022).

Over the past two decades, *C. elegans* has become a major model organism for the study of meiotic mechanism (Hillers, 2015). In *C. elegans*, the sperms and oocytes are produced in spermatogenesis and oogenesis, which both take place through the process of meiosis. During spermatogenesis, the primary spermatocyte cells give rise to four spermatids cells after Meiosis II; while during oogenesis, the primary oocytes give rise to one ootid and three polar bodies (Libretexts, 2022).

1.1.2 Role of type II DNA Topoisomerases in meiosis

Eukaryotic type II DNA Topoisomerases are highly conserved in both structure and function (Holm et al. 1985; Drake et al. 1989; Ramos et al. 2011). In lower eukaryotes and invertebrates, only a single type of type II topoisomerase, topoisomerase II (Topo II), is encoded; while vertebrate species encode two closely related isoforms, topoisomerase II α and topoisomerase II β (Deweese & Osheroff, 2009). In *C. elegans*, topoisomerase II exists as a large ATP-dependent, homodimeric enzyme. Each

protomer subunit of type II DNA Topoisomerases creates a transient break on one DNA strand, translocates a second unbroken strand through the break, and then rejoins the break (Nitiss, 2009). All topoisomerases contain active site tyrosyl residues in order to catalyze DNA cleavage and ligation (Deweese & Osheroff, 2009). The active site tyrosine works as a nucleophile that attacks the nucleic acid backbone phosphate. This nucleophilic attack results in cutting the DNA strand by forming a phosphotyrosyl bond that links the enzyme to the newly generated 5'-terminus of the DNA chain (Figure. 1). Unlike type I topoisomerases, which only cut a single DNA strand, type II DNA Topoisomerases cleave both DNA strands. Also, ATP is needed as the energy source for type II DNA Topoisomerases to complete the catalytic activity (Hamiche et al., 1999).

C. elegans type II DNA topoisomerase (Topo II) is encoded by the gene *top-2* located on chromosome II. Topo II is an ATP-dependent enzyme that alleviates DNA tangles and supercoils during transcription by cutting both DNA strands simultaneously (Nitiss, 2009). The role of Topo II in meiosis is critical and highly conserved among organisms like mammals, yeast, *Drosophila*, and *C. elegans* (Rose and Baillie 1980; Hartsuiker et al. 1998; Li et al. 2013; Hughes and Hawley 2014; Mengoli et al. 2014; Jaramillo-Lambert et al. 2016). A specific mutation of the *C. elegans top-2* gene, *top-2(it7ts)*, causes disruption in homologous chromosome segregation during Meiosis I and embryonic lethality (Jaramillo-Lambert et al. 2016). *top-2(it7)* is a temperature-sensitive allele, which contains a missense mutation (arginine to cysteine amino acid change), within the catalytic domain of TOP-2. This

arginine is highly conserved among organisms and is located within the “tower domain” of the enzyme, which indicates it possibly has a critical role in DNA binding. When cultured at 24°C since the L4 stage, the hermaphrodites are not capable in producing viable progeny compared to when cultured at 15 °C. Disruption of chromosome segregation during spermatogenesis due to high temperature results in anucleate sperm and embryonic lethality after fertilization (Jaramillo-Lambert et al. 2016).

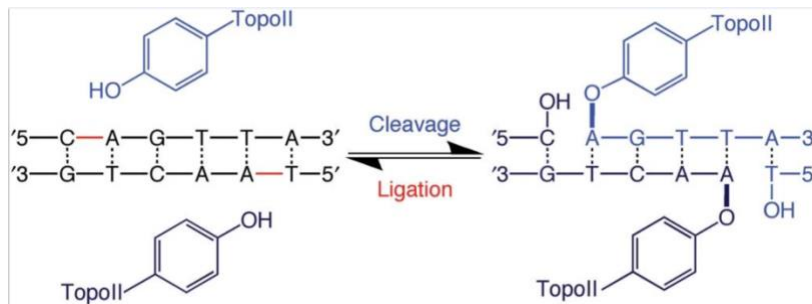


Figure 1. Double-stranded DNA cleavage and ligation catalyzed by topoisomerase II. During cleavage, the active site tyrosine from each subunit covalently links to the 5' terminal phosphate group on the opposite strands four bases apart. Ligation is the reverse of the process and does not change the chemical structure of the DNA strands. Diagram retrieved from Dewese & Osheroff, 2009.

1.1.3 Why do we study *nurf-1*?

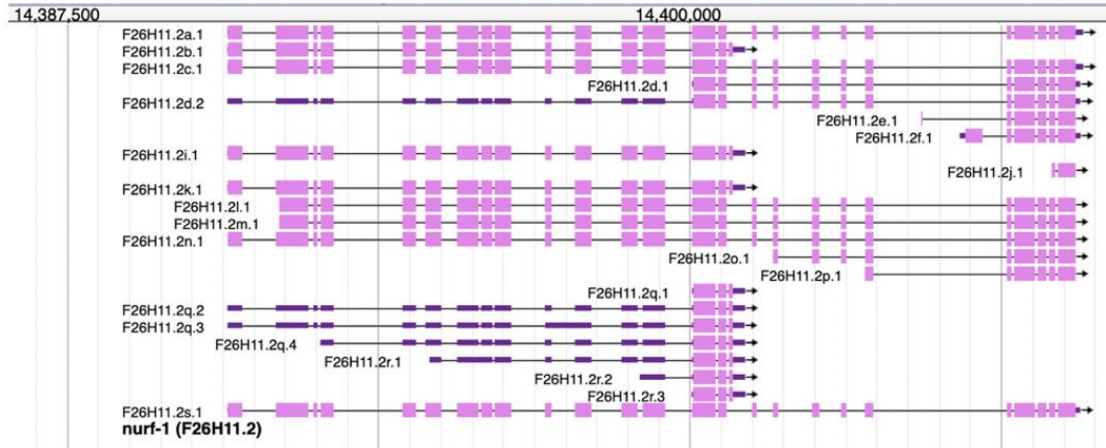
In 2020, 11 lines of missense mutations were discovered to be able to rescue the *top-2(it7)*-induced embryonic lethality. Among the mutations, *mep-1(ude14)* [G57D] and *nurf-1(ude23)* [E1954K] were found to co-suppress *top-2(it7)* embryonic lethality (Bhandari et al., 2020). According to the data presented in their research, RNAi knockdown of the single candidate genes *mep-1(ude14)* [G57D] and another candidate *nurf-1(ude23)*[E1954K] were unable to rescue the embryonic lethality of *top-2(it7)* (1.0% and 1.7% embryonic viability respectively). Though neither of the two suppressors is considered suppressing *top-2(it7ts)* embryonic lethality individually, the combined RNAi knockdown of both suppressor genes had 9.2% viable progeny and is considered to co-suppress the *top-2(it7)*-induce embryonic lethality (Bhandari et al., 2020). Since both *mep-1* and *nurf-1* are involved in chromatin remodeling, it is assumed that their gene products might work interactively in intervening the disruption of chromosome segregation during Meiosis I. Yet, the mechanism in this co-suppression remains unknown. Also, whether the missense mutation in either suppressor gene (*nurf-1* or *mep-1*) alone will cause a phenotype in oogenesis or spermatogenesis (or both) also remains unknown. My research focuses on examining the role of *nurf-1* in regulating chromosome segregating during meiosis I and observing the possible effect that *nurf-1(ude23)* [E1954K] has on oogenesis or spermatogenesis.

Nucleosome Remodeling Factor (NURF) protein in *Caenorhabditis elegans*, NURF-1, is encoded by the *nurf-1* gene (F26H11.2) on chromosome II. NURF-1

protein has 17 different isoforms (Fig.2a). The longest *nurf-1* coding sequence is 6751 bp, and the shortest coding sequence is 435 bp (Andersen et al., 2006). The *C. elegans* NURF-1 protein is highly conserved among eukaryotes and has well-studied orthologs, such as the *D. melanogaster* NURF301 subunit and the *Homo Sapien* Nucleosome Remodeling Factor subunit BPTF (Barak et al., 2003). NURF-1 is predicted to be part of NURF complex, which belongs to the ISWI family of chromatin remodeling complexes (Andersen et al., 2006). NURF complexes play a critical role in regulating transcription, establishing boundary elements, and promoting higher order of chromatin structure (Alkhatib & Landry, 2011). The detailed mechanism of NURF-1 in transcription regulation and chromosome remodeling remains unknown, however, it is indicated that NURF-1 might be involved in enabling of RNA polymerase II cis-regulatory region sequence-specific DNA binding activity (Andersen et al., 2006) and modifying the methylated histone binding activity (Wysocka et al., 2006).

The *C. elegans* gene *nurf-1* was first curated in 2004. Two most common mutant alleles used in research labs are *n4293Δ* with a 724 bp deletion at the splice donor region of exon 1 and it removes all of exon 1 (Fig.2b), and *n4295* with 1077 bp deletion at the 3' end of F26H11.3 (Andersen et al., 2006). In my research, the heterozygous strain MT13664 (Table S1) was used to characterize the *n4293Δ* allele. Previous study of the deletion in *n4293Δ* found that the deletion leads to homozygous sterility through suppression of normal protein production, specifically affecting the *nurf-1* isoform a (Andersen et al., 2006).

A.



B.

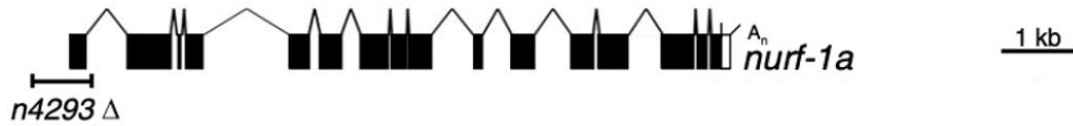


Figure 2. The *nurf-1* locus on chromosome II.

(A) 17 isoforms of *nurf-1* gene (F26H11.2); all isoforms are predicted to produce proteins with different functions. Diagram retrieved from wormbase.org. (B) Genomic structures of the isoform studied in this research, *nurf-1 a*. Mutant allele *n4293Δ* is presented as a 724 bp deletion at the splice donor region of exon 1 and it removes all of exon 1. Diagram retrieved from Andersen et al., 2016.

1.1.4 Possible role of NURF-1 in meiosis

The exact role of *C. elegans* NURF-1 in meiosis remains unknown. However, Nucleosome Remodeling Factor (NURF) protein is highly conserved both structurally and functionally in eukaryotes. Learning about the NURF-1 orthologs may lead the way for our future research on *C. elegans* NURF-1.

Two of the most studied NURF-1 orthologs are *Drosophila* NURF301 and human BPTF (Figure 3). NURF301 is one ATP-dependent subunit of the *Drosophila* NURF chromatin remodeling complex, which belongs to the ISWI family (imitation SWI; SWI stands for SWItch, component of the eukaryotic chromatin remodeling complex, SWI/SNF, or SWItch/Sucrose Non-Fermentable) (Alkhatib & Landry, 2011). NURF complex catalyzes the bidirectional “sliding” of neighboring nucleosomes through interacting with sequence transcription factors and acetylated histone octamers (Hamiche et al., 1999; Fig 4). The human NURF chromatin remodeling complexes also include the ATP-dependent NURF-1 ortholog, BPTF, which has similar functions in redistribution of the nucleosome arrays on chromatin and facilitating access to DNA during replication, transcription, and repair (Lazzaro et al., 2003).

In *C. elegans*, the NURF-1 protein encoded by *nurf-1* isoform a contains possible DNA-binding domains, an HMGY/I domain (Reeves and Beckerbauer, 2001), a DDT domain (Doerks et al., 2001) and a PHD finger (Schindler et al., 1993; Aasland et al., 1995). Its structure is believed to be most similar to the N terminus of NURF301 (Andersen et al., 2006). Studies using the *nurf-1* a deletion allele (*n4293Δ*)

showed that the mutants suppressed the synMuv phenotype and caused sterility (Andersen et al., 2006). It suggests that *nurf-1a* might be involved in co-acting with *isw-1*, which encodes an ATP-dependent chromatin remodeling protein, to promote the synMuv phenotype (Andersen et al., 2006). The ATP-dependent chromatin remodeling protein encoded by *isw-1*, ISW-1 (imitation SWI), is an ortholog of Drosophila ISWI, component in the Drosophila NURF complex along with NURF301, the *C. elegans* NURF-1 homolog, NURF38, and NURF55 (Alkhatib & Landry, 2011; Figure 3 left). The human SNF2L subunit is another ortholog of the *C. elegans* ISW-1, which forms the human NURF complex through interaction with BPTF, the human NURF-1 ortholog, and RBAP46/48 (Alkhatib & Landry, 2011; Figure 3 right). Nevertheless, whether *C. elegans nurf-1* has other roles during meiosis is unknown. Also, more research needs to be conducted to study what and how other genes may interact with *nurf-1* in regulating the chromatin remodeling pathway.

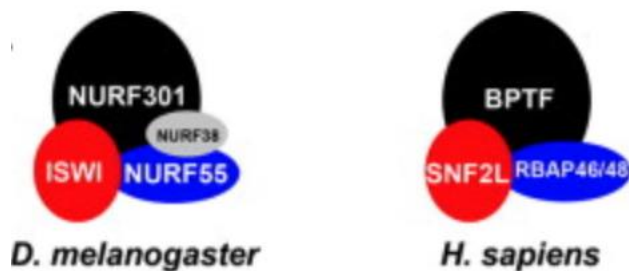


Figure 3. Structural components of NURF complex in *D. melanogaster* (Drosophila) and in *H. sapiens* (Human). Drosophila NURF complex contains the *C. elegans* NURF-1 ortholog NURF301 and ISWI subunits, co-acting NURF38 and NURF55 subunits. Human NURF complex contains the *C. elegans* NURF-1 ortholog BPTF, and co-acting subunits, SNF2L and RBAP46/48. Retrieved from Alkhatib & Landry, 2011.

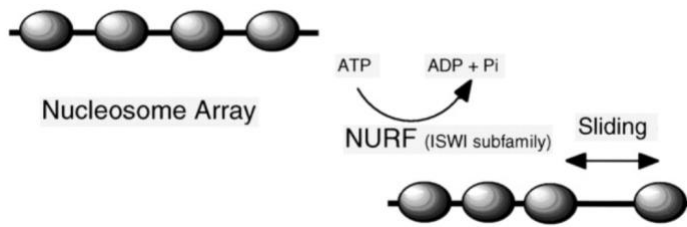


Figure 4. Possible mechanism of NURF complex in nucleosome regulation. NURF complex depends on ATP to cause a “sliding” effect between two neighboring nucleosomes and then expose the DNA region for replication, transcription, and repair. Retrieved from Hamiche et al., 1999.

1.2 *C. elegans* as model organisms

C. elegans are a type of nematode that are commonly used in the research labs as model organisms. They are transparent worms with an approximate average length of 1mm for adults and 0.25mm for the newly hatched larvae (Corsi et al., 2015). Most of the worms are maintained at the temperature of 20°C. Their average life span is about 25 days under 20°C (Huang, 2004). *C. elegans* exist mainly as hermaphrodites which are able to produce both sperm and oocytes and to self-fertilize. A much lower ratio of *C. elegans* exist in wild type as males ($\leq 0.2\%$) (Yin & Haag, 2019)

C. elegans became popular in research labs as model organisms for a few reasons. Firstly, *C. elegans* grow in large numbers in only a few days. One generation of worms are typically maintained in an approximate 3-day cycle, from L4 stage larvae until the next generation of L4 larvae. This allows quick notice of any effects from genetic changes in only a few days. Secondly, *C. elegans* are anatomically simple, and their transparent appearance allows easy observation of the fate of

individual cells using simple microscopy or staining techniques such as DAPI staining (Corsi et al., 2015). *C. elegans* only have 5 pairs of autosomes and 2 sex chromosomes in hermaphrodites or 1 sex chromosome in males. *C. elegans* hermaphrodites have two X chromosomes and *C. elegans* males only one X chromosome. This characteristic makes it easy to manipulate the sex when setting a genetic cross. Male worms could be produced from nondisjunction of the X chromosomes, which can be induced by a simple heat shock. In addition, it is much easier to map out all the genes in *C. elegans* genome than in humans. Eventually, the research on *C. elegans* may benefit studies involving human disease because *C. elegans* share many similarities at the molecular level with humans (Corsi et al., 2015).

1.3 Research Goal

As mentioned in the research from Bhandari et al 2020, *mep-1* and *nurf-1* are found to interact genetically as co-suppressors of the *top-2(it7)*-induced lethality. To study the possible mechanism behind this co-suppression, my research focuses on understanding the role of *nurf-1* in meiosis in the absence of the *top-2(it7)*-mutation. In this study, two different types of mutations are used and compared, deletion (*n4293Δ*) and single missense mutation *nurf-1(ude34)* [E1952K]. The *n4293Δ* deletion was 725bp and removes the whole exon 1, it was also previously shown to cause sterility in homozygous mutant worms (Andersen et al., 2006), while the effect caused by the E1952K missense mutation was unknown.

In this study, the mutants were characterized based on the observable phenotypes of different genotypes. This characterization was done in two methods in my study: measurement of the fertility of each genotype by performing an embryonic viability assay and calculating the viable progeny; observation and comparing the phenotypes on the gonads in adult hermaphrodites and males in each genotype by DAPI staining and imaging. In addition, the suppressor gene *nurf-1*[E1952K] was recreated using CRISPR/Cas9 genome editing. Since *n4293Δ* contains a deletion that removes the whole exon 1 on *nurf-1*, my hypothesis was this deletion would have observable phenotypes including defects in germline cells and incapability in producing viable progeny. For the CRISPR-induced single missense mutation *nurf-1(ude34)* [E1952K], I hypothesize that it would also cause a phenotype in germline cell defects, as well as incapability in producing viable progeny or could only produce

much less amount of viable progeny. The Embryonic Viability Assay (EVA) was scored on not only the mutant homozygous hermaphrodites from *n4293Δ* and from *nurf-1(ude34)* [E1952K], but also on the hermaphrodites from the control groups: the heterozygous that only carry one *n4293* deletion allele (*n4293Δ/mnC1*) as well as N2 wildtype. The results confirmed the sterility in the homozygous *n4293Δ*. However, my hypothesis about the CRISPR-induced single missense mutation *nurf-1(ude34)* [E1952K] was not supported by its result from the embryonic viability assay. The count of progeny from the homozygous *ude34* did not show significant difference from the N2 strain (WT group) or the control group. This indicates that the single missense mutation of Glutamate to Lysine at position 1952 does not have any impact on the fertility in *C. elegans* hermaphrodites. This conclusion is also supported by the results from whole-mount DAPI staining of hermaphrodites and males in both genotypes. The DAPI images of the homozygous *n4293Δ* hermaphrodites showed significant defects in embryogenesis, which might explain its sterility phenotype. In contrast, The DAPI images of the homozygous *ude34* hermaphrodites did not show any observable defects in the germline cells nor embryos. Referring to the study of the suppressors to the *top-2*-induced embryonic lethality, the single missense mutation *nurf-1(ude23)* [E1954K] was discovered as a co-suppressor to another single missense mutation *mep-1 (ude14)* [G57D]. Together, they could rescue the *top-2*-induced embryonic lethality by 9.2% (Bhandari et al., 2020). A possible co-suppression mechanism might exist from the interaction between *nurf-1* and *mep-1*. Hence, further study will be necessary in combining these two single missense mutations, as well as

characterization of the combination and how could they interact with *top-2* to suppress the embryonic lethality.

Chapter 2

MATERIALS AND METHODS

2.1 Strains

C. elegans strains are listed in Table S1 and all cultured under standard conditions (Brenner, 1973).

2.2 Embryonic Viability Assay

The animals used in the embryonic viability assay include the genotypes of N2, *nurf-1(n4293Δ)/mnC1*, *nurf-1(n4293Δ)*, and the CRISPR-induced line *nurf-1(ude34)* [E1952K]. Individual L4 hermaphrodite larvae were placed on a single 35 mm MYOB plate spotted with 50 μL of OP50 *E.coli* bacteria culture. Each hermaphrodite was left to mature and to lay embryos at 20°C for a 24 hr period. Adult worms were then transferred to fresh plates every 24 hours until no additional embryos were produced. The number of laid embryos and hatched larvae were counted. Calculations for percent hatching were done as the number of hatched larvae divided by the total number of embryos laid.

2.3 Whole-mount DAPI Staining

Individual L4 hermaphrodite larvae were picked and incubated at 20°C for 24 hours. The animals were then prepared for whole-mount worm fixation using methanol. 20 animals were picked into 5 ml of M9 minimal medium (M9) on a regular

glass slide. All M9 was wicked away with a Kimwipe, then 15 ml of 100% room temperature methanol was added to the animals on the slide. 12 ml of DAPI solution (2 mg/ml in water) was added immediately on the fixed animals once the methanol evaporated (in about 30 seconds). A coverslip was added right away onto the animals in DAPI and then sealed with clear nail polish. Each slide was incubated in darkness for at least 30 mins prior to imaging.

Collection of images was obtained using a Zeiss AXIO Observer microscope (Carl Zeiss, Inc., Gottingen, Germany) under 40X magnification. Images were stitched and processed using Fiji Is Just ImageJ (Fiji) (Schindelin et al. 2012). Brightness and contrast were adjusted for better visualization.

2.4 CRISPR/Cas9-Mediated Genome Editing and Screening

CRISPR/Cas9-Mediated Genome Editing was performed to create the *nurf-1(ude34)* [E1952K] mutation in N2 strain via the clone-free method (Paix et al. 2015) and the use of *dpy-10* as a co-CRISPR marker (Arribere et al. 2014). First, an injection mix of Cas9 protein (25 mg), *dpy-10* crRNA (3.2 mg, Dharmacon, GE Life Sciences, Pittsburgh, PA), *dpy-10(cn64)* repair oligonucleotide (0.2 mg), universal tracrRNA (20 mg, Dharmacon), an allele-specific crRNA (8 mg) and a gene-/allele-specific repair oligonucleotide (3.8 mg) was made, centrifuged for 6 mins under maximum speed, and then incubated at 37°C for 15 mins. To recreate the point mutation that changes Glu 1952 to Lys, a crRNA targeting the sequence

GAGCTGTGAGGAATGTATTGAGG was used, along with a repair template

(TGGGTTTGGAGCACTGGAGCTGTGAGGAATGTATTTAAAGAGCAGGAGAGAGTCAAGGATCAGCCGGCGTTGTA) with sequence to edit codon 1952 (bold), and a MseI recognition site (underlined) for genotyping.

Before the injection, N2 L4 hermaphrodite larvae were picked and incubated at 20°C for 24 hours. Next, the prepared mix was injected into the gonad of each N2 worm. After injection, the individual worm was rehydrated in M9 and then placed on a single 35 mm MYOB plate seeded with OP50. The animals (P0) were then incubated at 20°C and allowed to produce progeny until the screening step (Kim & Colaiácovo, 2019).

For the screening step, every rolling F1 progeny was identified and picked onto a fresh plate. The phenotype of rollers indicates an active Cas9 and *dpy-10* sgRNA was present in the germ line of the injected P0. F1 rollers are *dpy-10/+* and potentially *nurf-1/+*. Once F1 rollers laid about 25-50 embryos, the P0 worm was lysed for genotyping. The lysates were then used as template in running a PCR, a digest, and then imaging on an agarose gel. According to the result after gel imaging, only plates containing heterozygotes or homozygotes were kept and maintained for further analysis. Later, F2 L4 non-dpy/non-roller hermaphrodites were transferred to fresh plates and allowed to lay F3 embryos. The F2 worms were made into single worm lysates and the plates genotyped in the same way as the F1 generation. The genotype of potential homozygous F2 animals was verified via sequencing of the PCR product. See Figure 5 for details.

CASPR/Cas9 Genome Editing in *C. elegans*

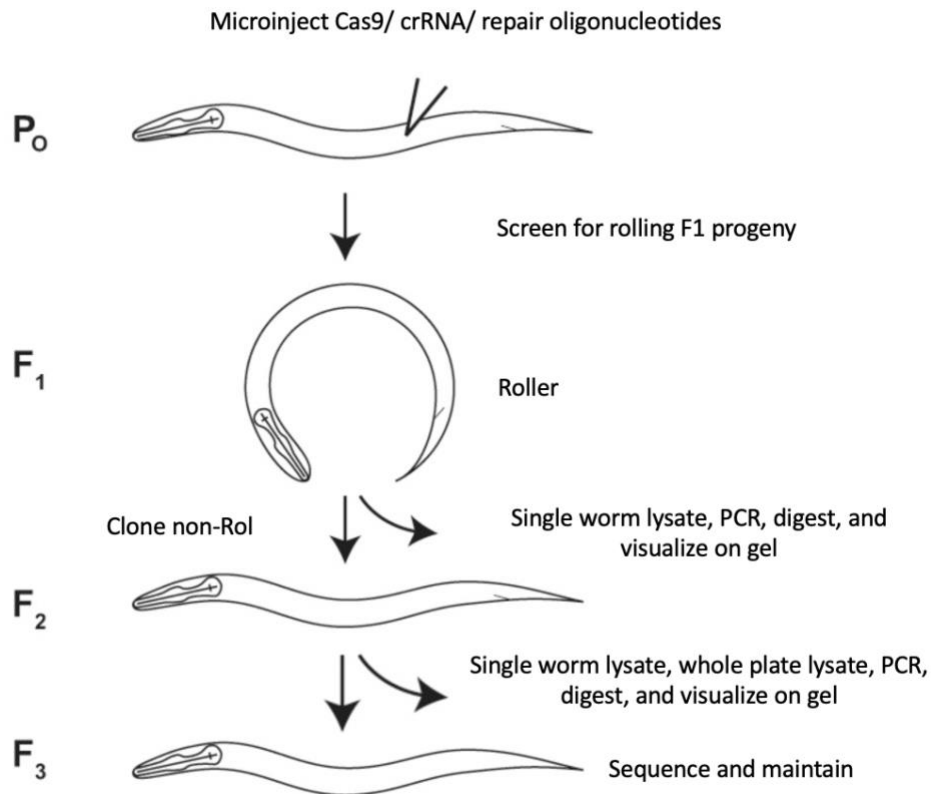


Figure 5. CRISPR/Cas9 Genome Editing in *C. elegans*. Injection was done with an injection mix of Cas9 protein, *dpy-10* crRNA, *dpy-10(cn64)* repair oligonucleotide, universal tracrRNA, *nurf-1*-specific crRNA and *nurf-1*-specific repair oligonucleotide. Rollers were picked and allowed to produce embryos in F1 generation before proceeded to make into single worm lysates. Single worm lysates of F1 rollers then went through PCR, enzymatic digest, and finally visualized on agarose gel. In the F2 generation, heterozygous or homozygous non-rollers were picked, lysed, and processed using the same procedure. Finally, selected F3 worms were sequenced to confirm the induced point mutation. F3 plates were maintained under standard conditions.

2.5 Creation of the *nurf-1*; *him-8* line

Males spontaneously arise in populations of hermaphrodites through chromosome nondisjunction (Anderson & Phillips, 2010). Heat shocking worms is one method of inducing chromosome nondisjunction. 5-10 L4 hermaphrodites were picked and incubated for 4-6 hours at 30°C. After the heat shock, 2-5% of males could be obtained in the F1 generation. In this study, the homozygous *ude34* males used in the whole-mount DAPI staining were obtained as F1 progeny after 6 hours heat shock of the *nurf-1(ude34)* [E1952K] plates.

Another method for increasing males in a population is the introduction of a genetic mutation that increases the rate of X chromosome nondisjunction. For this method, *him-8(e1489)* allele, which produces ~30% males, is genetically crossed with the strain of interest for a higher ratio of males. To create the *nurf-1(n4293Δ)*; *him-8(e1489)* line, first, *him-8(e1489)* IV males was crossed with *unc-4(e120)/mnC1 [dpy-10(e128) unc-52(e444) umnIs32]* II hermaphrodites. The male F1 progeny with GFP fluorescence [*mnC1-GFP* /+; *him-8(e1489)* /+] were picked and then crossed with the *nurf-1(n4293Δ)/mnC1 [dpy-10(e128) unc-52(e444)]* II hermaphrodites. The WT hermaphrodite progeny [*nurf-1(n4293Δ)/mnC1-GFP*; *him-8(e1489)* /+ or *nurf-1(n4293Δ)/ mnC1-GFP*; +/+] with GFP fluorescence in F2 were picked and allowed self-cross to produce embryos. In the F3 generation, individual WT hermaphrodite progeny with GFP fluorescence were picked to single plate and allowed self-cross. The plates containing male F4 progeny were selected and maintained [*nurf-*

1(n4293Δ)/ mnC1-GFP; him-8(e1489)/him-8(e1489)]. See Figure 6a for details. The *nurf-1(ude34)* [E1952K]; *him-8(e1489)* line was also created by crossing with the homozygous *him-8(e1489)* males. First, *unc-4(e120)/mnC1 [dpy-10(e128) unc-52(e444) umn1s32]* II hermaphrodites were crossed with *him-8(e1489)* IV males to obtain males in F1 progeny with GFP fluorescence [*mnC1-GFP* /+; *him-8(e1489)*/+]. Then the GFP males from F1 were crossed with the homozygous CRISPR-induced *nurf-1(ude34)* [E1952K] hermaphrodites. Hermaphrodites with GFP in F2 [*nurf-1(ude34)*[E1952K]/*mnC1-GFP*; *him-8(e1489)*/+ or *nurf-1(ude34)*[E1952K]/*mnC1-GFP*; +/+] were picked and allowed self-cross. In F3, non-GFP hermaphrodites were picked to obtain the homozygous genotype of *nurf-1(ude34)*[E1952K]/*nurf-1(ude34)*[E1952K]. These non-GFP hermaphrodites were cultured in 60 single worm plates and allowed self-cross. In F4, plates with male progeny [E1952K]/*nurf-1(ude34)* [E1952K]; *him-8(e1489)/him-8(e1489)* were maintained. (Figure 6b.) To confirm that the single missense mutation E1952K was still present, a whole plate lysis was performed on F4 progeny, then PCR amplification and enzymatic digest from MseI. The final result was visualized via gel electrophoresis, and the existence of the single missense mutation E1952K was confirmed (Figure. 6c).



(a)

Figure 6. Genetic cross procedure to obtain males using *him-8(e1489)* line.

(a) Creation of *nurf-1 (n4293Δ)*; *him-8(e1489)* line that produce male progeny. In F2 progeny, *mnC1/mnC1::GFP* has the phenotype of being paralyzed. Hence the only genotype that carrying the GFP phenotype without looking paralyzed was *n4293Δ/mnC1::GFP*. F3 hermaphrodite with GFP were cultured in 40 single worm plates and allowed self-cross. Only plates with male progeny [indicating presence of homozygous *him-8(e1489)*] were maintained. (to be continued...)



(b)

Figure 6. cont. (b) Creation of *nurf-1 (ude34)[E1952K]; him-8(e1489)* line that produce male progeny.

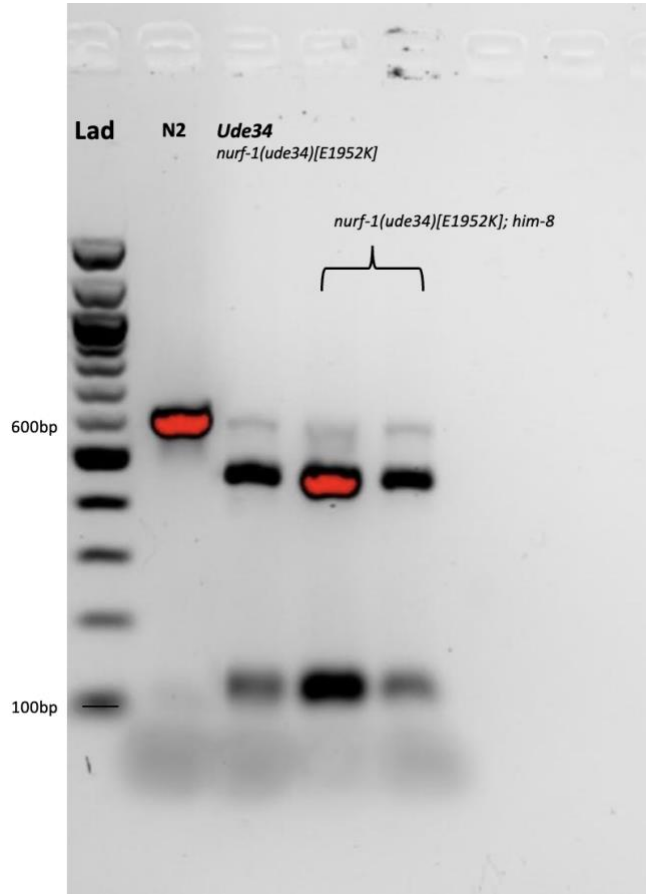


Figure 6. cont. (c) To confirm the remaining of the single missense mutation E1952K, whole plate lysis was performed on the F4 progeny, followed by PCR amplification and MseI enzymatic digest. The result of digestion was finally visualized through gel electrophoresis. May be put figures 6 A-C in one figure with three panels.

(c)

Table S1. Strains used in this study.

Strain Name	Genotype
20 °C N2 MT13664 CB1489 CGC43 AJL67	wild-type Bristol isolate <i>nurf-1(n4293Δ)/mnC1 [dpy-10(e128) unc-52(e444)] II; lin-15B&lin-15A(n765) II.</i> <i>him-8(e1489) IV</i> <i>unc-4(e120)/mnC1 [dpy-10(e128) unc-52(e444) umnIs32] II</i> CRISPR-induced <i>nurf-1(ude34)[E1952K]/nurf-1(ude34)[E1952K]</i>
Male-producing lines obtained from genetic cross:	
AJL68	<i>nurf-1(n4293Δ)/mnC1 [dpy-10(e128) unc-52(e444)] II; lin-15B&lin-15A(n765); him-8(e1489)/him-8(e1489)</i>
AJL71	<i>nurf-1(ude34)[E1952K]/nurf-1(ude34)[E1952K] him-8(e1489)/him-8(e1489)</i>

Chapter 3

RESULTS

3.1 Successful recreation of the *nurf-1*[E1952K] suppressor allele using CRISPR/Cas9 genome editing

nurf-1(ude23) [E1954K] was discovered as one of the suppressor alleles of the *top-2(it7)*-induced embryonic lethality (Bhandari et al., 2020). Multiple isoforms exist for the *nurf-1* gene, the recreation of *nurf-1* suppressor allele was designed to contain a single point mutation on E1952K instead. The original amino acid Glutamate (**GAG**) on position 1952 was replaced with a Lysine (**AAA**). CRISPR/Cas9 genome editing was performed on N2 adult worms to induce the desired single point mutation. To test whether the injection was successful, F1 progeny with a rolling phenotype (rollers) were searched and screened. 36 F1 rollers were found from three out of 10 P0 worms, and were labeled as #1, #5, and #9. The F1 rollers were lysed as single worms to expose their genetic material, then went through polymerase chain reaction (PCR) to amplify the target DNA region, and MseI enzymatic digest to recognize and cut at the designed site of mutation. Next, the digested DNA fragments were visualized on an agarose gel via gel electrophoresis. As shown in Figure 7(a), four rollers showed signs of being completely or partially digested (roller 1.2; 9.6; 9.24; and 5.2). The length of the DNA fragment to be amplified was 607 base pair (bp), and the digested fragments were expected to be 471 bp and 136 bp. The F2 progeny of these four rollers were then screened through the same procedures to identify worms homozygous for the

edit. Analysis of digested F2 whole plate lysates from the mentioned four F1 rollers showed that some of the F2 progeny were homozygous WT, some were heterozygous for the genome edit, and some were potentially homozygous for the edit [Figure 7(b)]. Four of the F2 non-roller worms (numbered as 5.2.6; 9.6.1; 9.6.2; and 9.24.2) were considered as homozygous for the desired point mutation Figure 7(c). Later, a whole plate lysis and same screening procedures were performed on F3 progeny from these four F2 worms to confirm their homozygosity (see Figure 7d). All four non-roller worms exhibited possible homozygosity.

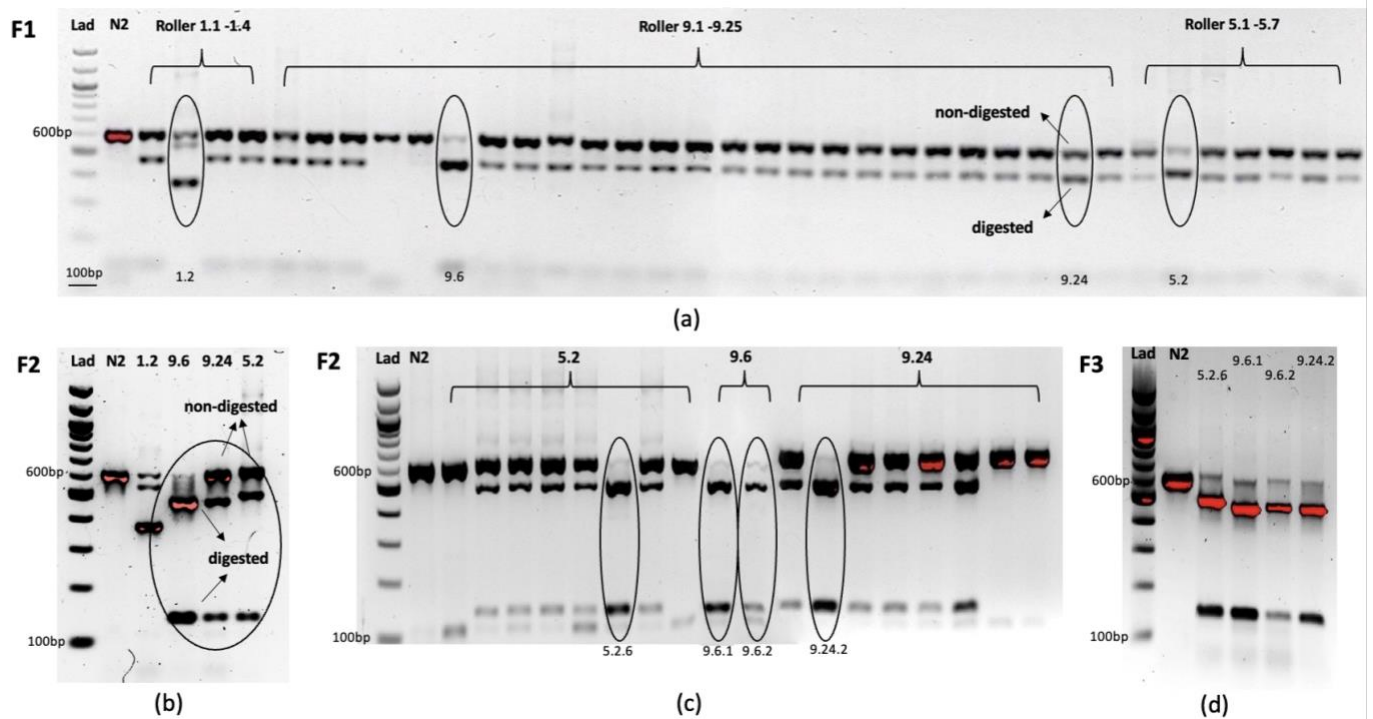


Figure 7. Gel images of the MseI enzymatic digest results on F1, F2, and F3 worms after CRISPR/Cas9 genome editing on N2 worms. Non-digested bands and digested bands are shown with arrows. (a) Analysis of 36 F1 rollers. Lanes with complete or partial digestion are circled. (b) Analysis of F2 progeny from the circled F1 rollers (whole plate lysates). F2 progeny from roller 9.6 exhibits possible homozygosity, while progeny from roller 9.24 and roller 5.2 exhibit possible heterozygosity. (c) Analysis of non-roller F2 progeny from the circled F1 rollers (single worm lysates). The circled four worms exhibit possible homozygosity. (d) Analysis of F3 progeny from the circled F2 worms (whole plate lysates). All exhibit possible homozygosity.

3.2 *nurf-1* [E1952K] allele does not cause embryonic lethality

To determine if *nurf-1* mutations have meiotic defects, I performed embryonic viability assays (EVA) as shown in Figure 9. For all the measured genotypes, only hermaphrodites were scored. Hermaphrodites of N2 and *nurf-1(n4293Δ)/mnC1* were used as control groups. The average percent viability in N2 was scored as 99.6%, while in *nurf-1(n4293Δ)/mnC1* was 99.1%. There was no significant difference between these two genotypes. The CRISPR/Cas9-mediated recreation of suppressor allele, homozygous *nurf-1(ude34)* [E1952K], showed wildtype phenotype capable of producing viable progeny with an average percent embryonic viability of 99.3%. This result represented no significant difference compared to N2. However, the homozygous mutants with a 724 bp deletion, *nurf-1(n4293Δ)*, was sterile with 0% viable progeny produced and no embryos laid. *nurf-1(ude34)* [E1952K] hermaphrodites were able to produce viable progeny (99.3%) just as N2 (99.6%) and the heterozygous genotype, *nurf-1(n4293Δ)/mnC1* (99.1%). This suggests that the single point mutation E1952K in *nurf-1* does not cause embryonic lethality.

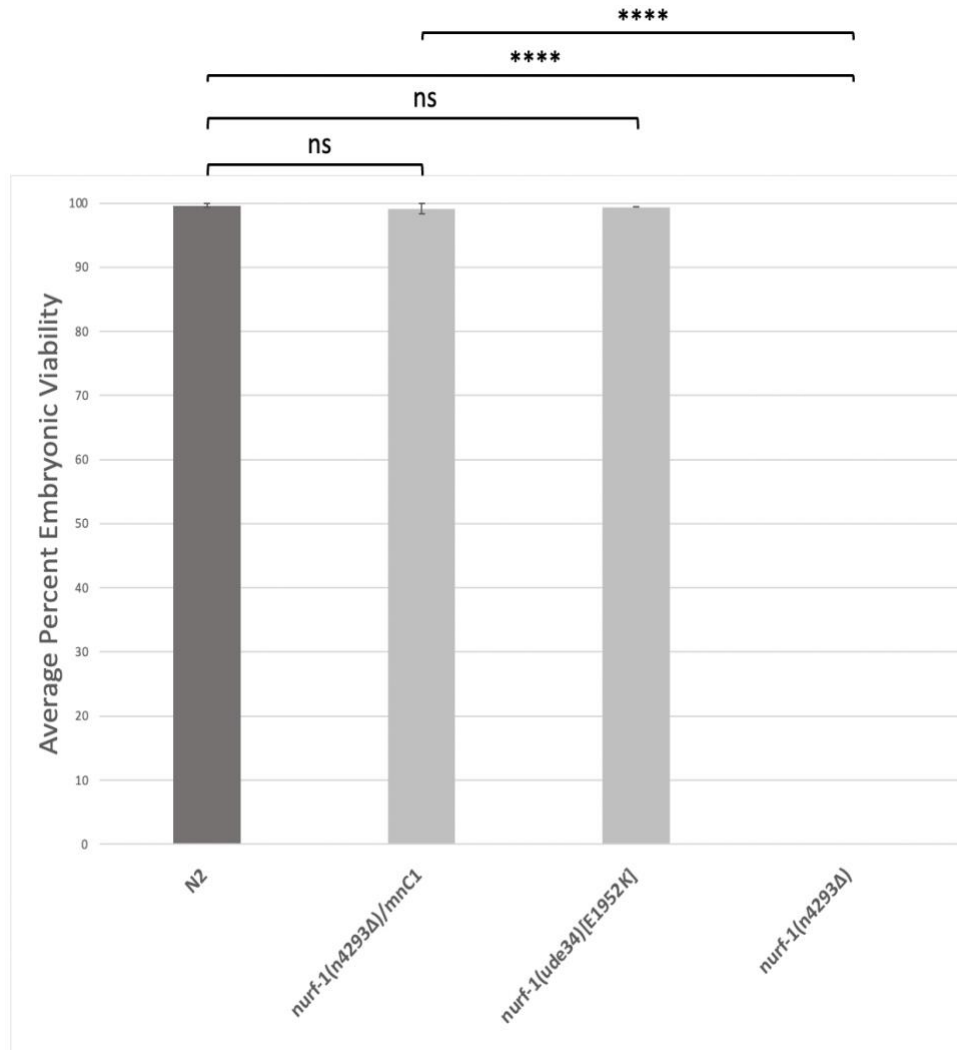


Figure 9. Average percent embryonic viability in N2 and *nurf-1* mutant hermaphrodites at 20°C. From left to right: N2: WT control line; SD=0.3.

nurf-1(n4293Δ)/mnC1: heterozygous control line; genotype with one mutant allele carrying a 724bp deletion; non-sterile; SD=0.8; p=0.135.

nurf-1(ude34) [E1952K]: homozygous CRISPR-recreated line; non-sterile; SD=0.1; p=0.09.

nurf-1(n4293Δ): homozygous genotype with a 724 bp deletion on both alleles; sterile; SD=0; p=2.92E-24 (significant to N2 line); p=6.93E-14 (significant to heterozygous control line *nurf-1(n4293Δ)/mnC1*)

Error bars on top of the columns indicate standard deviation of at least three independent experiments. The progeny of at least 30 hermaphrodites were scored for each genotype. SD: standard deviation.

n: total number of hermaphrodites scored.

p: statistical significance, two-tailed distribution, heteroscedastic.

ns: not significantly different; $p \geq 0.05$

****: significantly different; $p \leq 0.0001$.

3.3 Characterization of the *nurf-1(ude34)* [E1952K] allele

To characterize the effects of *nurf-1* mutations on meiosis, whole mount DAPI staining was performed on both hermaphrodites and males of *nurf-1(n4293Δ)/mnC1*, *nurf-1(n4293Δ)*, and the CRISPR/Cas9-mediated recreation of the suppressor *nurf-1* [E1952K] mutation [*nurf-1(ude34)*]. The heterozygous genotype, *nurf-1(n4293Δ)/mnC1*, was used as a control line for comparing to the homozygous *nurf-1(n4293Δ)* mutant with a 724bp deletion. DAPI (4',6-diamidino-2-phenylindole) binds to dsDNA at AT regions and exhibits a strong blue-fluorescence under microscopy (Kapuscinski, 1995). It is commonly used in studies on fixed *C. elegans* to visualize the germline nuclei and characterize germline phenotypes.

As depicted in Figure 11 (a), WT *C. elegans* hermaphrodites contain two U-shaped gonads, that extend from the dorsal side to the ventral side where the oocytes, the sperm, and the eggs are located near the vulva. WT males contain only one gonad that extends from the ventral side to the dorsal posterior side where the sperm are located. The results from DAPI staining of each genotype depicted the WT phenotype of the heterozygous group (control) as well as the CRISPR-induced mutants with the single point mutation E1952K. No germline defects were observed in either hermaphrodites or males in the CRISPR-recreated line (Figure 10). However, in *nurf-1(n4293Δ)*, defects were observed in the proximal gonad where embryos are formed in 28/30 hermaphrodites observed. Nevertheless, no significant defect in sperms or oocytes was detected. This indicates that the EVA confirmed phenotype of sterility does not come from the process of meiosis. The sterility phenotype may come from

defects in fertilization or defects in embryogenesis. The ratios of germline defects in each genotype were scored and compared in Figure 11 (b).

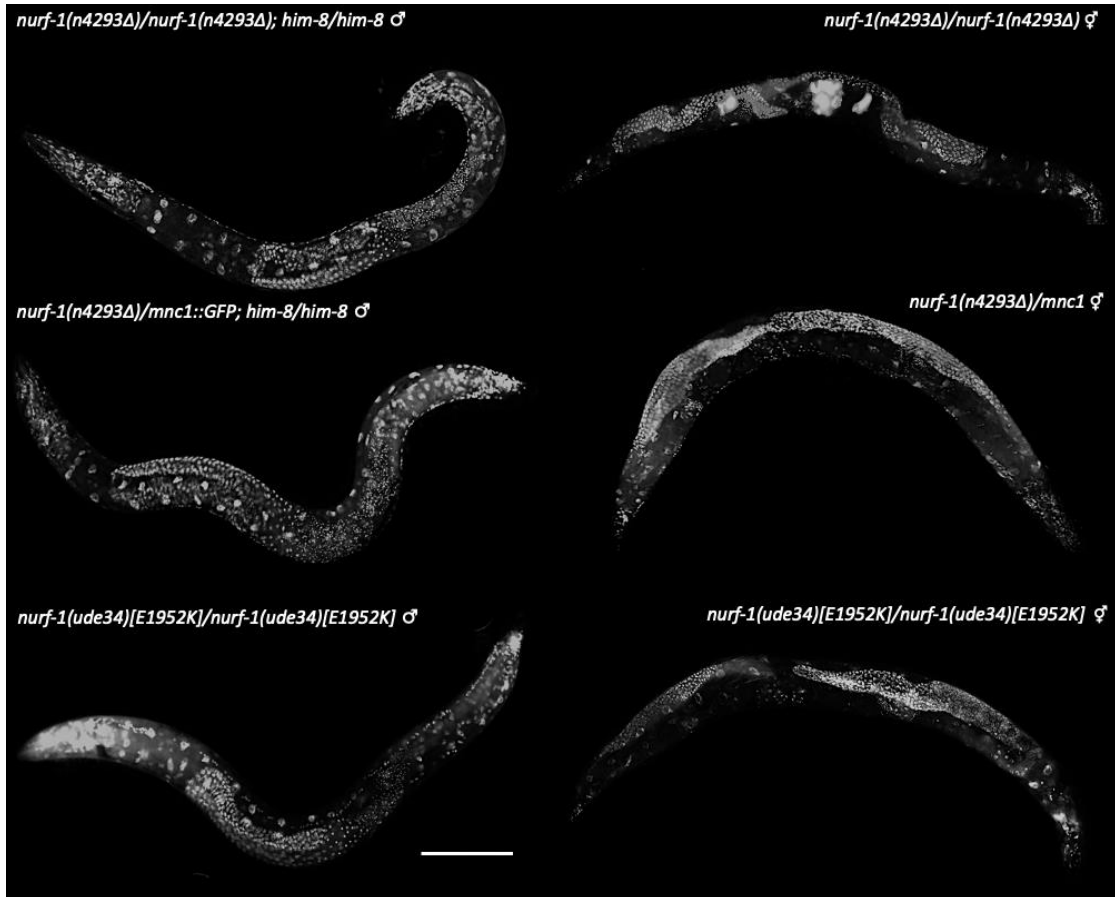
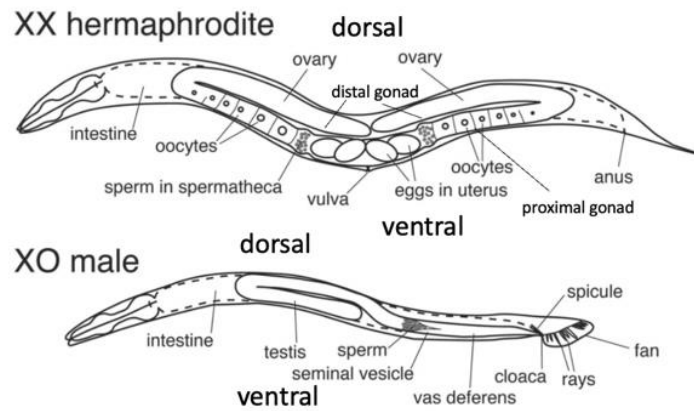


Figure 10. Characterization of *C. elegans nurf-1* mutations. Whole-mount DAPI staining images. Top: homozygous *nurf-1(n4293Δ)* males and hermaphrodites. No germline defect was observed in males. In hermaphrodites, no defect observed in sperms or oocytes. However, a significant portion of the worms showed defected embryos in the region near the vulva. This indicates a possible defect in fertilization or embryogenesis. Middle: heterozygous *nurf-1(n4293Δ)/mnc1* control males and hermaphrodites. Meiosis proceeds normally in these germlines. Bottom: homozygous *nurf-1(ude34)[E1952K]* males and hermaphrodites. No defect in sperms, oocytes, or embryos observed. More than 30 worms in each genotype were fixed and stained 24 hours after the L4 stage. Scale bar=100 μm.



(a)

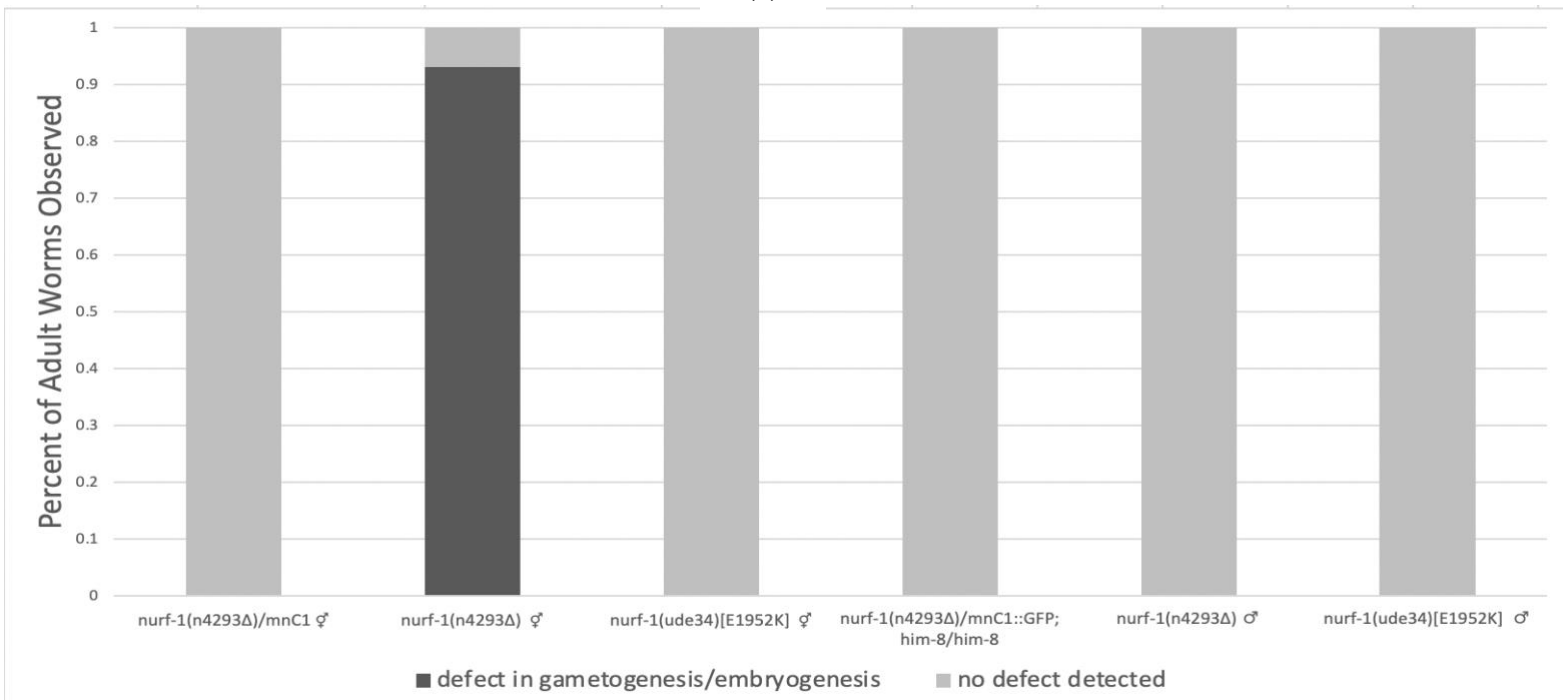


Figure 11. Reproductive systems in *C. elegans* and score of germline defects in adult worms of each genotype in this study. Homozygous *nurf-1(n4293Δ)* hermaphrodites showed significant defects in embryogenesis. (b) Cartoon drawing of *C. elegans* gonads of WT hermaphrodites and males. Adapted from wormbook.org. (c) Percent of germline defects in adult worms of each genotype. Heterozygous *nurf-1(n4293Δ)/mnC1* males and hermaphrodites were used as the control group for comparison. For each genotype, 30 adult worms were counted. 28/30 of the homozygous *nurf-1(n4293Δ)* hermaphrodites showed defects. For homozygous *nurf-1(n4293Δ)* males, 0/30 showed defects in the germline. For the CRISPR-created homozygous *nurf-1(ude34)* [E1952K] males and hermaphrodites, 0/30 showed observable germline defect.

Chapter 4

DISCUSSION

4.1 The Co-suppression mechanism of the *top-2-induced* embryonic lethality from *nurf-1* and *mep-1* remains unknown

Previous discovery and characterization of the temperature-sensitive mutant strain *top-2(it7ts)*, anucleate sperm were found in the germline cells leading to embryonic lethality after fertilization (Jaramillo-Lambert et al. 2016). Using the whole genome sequencing (WGS) method to identify the mutation, a single missense mutation at R828C in *top-2(it7ts)* was found in the catalytic “tower” domain, which is believed to be involved in DNA binding (Jaramillo-Lambert et al. 2016). However, how this single missense mutation affects TOP-2 enzymatic activity at the molecular level remains unknown. In addition, how this possible defect in TOP-2 function interferes with germ-line proliferation in both males and hermaphrodites, especially during late stages of meiotic prophase, also remains unknown (Jaramillo-Lambert et al. 2016). To identify meiosis-specific genes/pathways that interact with *top-2* we performed a genetic suppressor screen. So far, 11 suppressors were found to be capable in rescuing the *top-2*-induced embryonic lethality, which include *nurf-1(ude23)[E1954K]* and *mep-1(ude14)[G57D]* as co-suppressors (Bhandari et al., 2020). However, none of the mechanisms of suppression have been identified yet.

In this study, I characterized the *nurf-1* gene and its role as a suppressor of *top-2(it7)*-induced embryonic lethality. The *nurf-1* gene encodes a nucleosome-remodeling

factor subunit, which includes a variety of protein domains and regions, such as zinc-fingers, DDT domains, and bromodomains (AlphaFold, 2022). The DDT domain (DNA-binding homeobox-containing proteins and the Different Transcription and chromatin remodeling factors) is a domain of about 60 amino acids. It is characterized by a number of conserved aromatic and charged amino acids and is predicted to consist of three α helices. The DDT domain is believed to have a function in DNA-binding (Doerks et al., 2001). As seen in Figure 12 (a), the wildtype *nurf-1* gene encodes the amino acid Glutamic acid at position 1952, which is within a predicted short DDT domain (1948-2014) in between two zinc fingers (1899-1950; 1959-2010). Using CRISPR-Cas9 genome editing, we induced a single missense mutation from this Glutamic acid (1952), which carries a negative charge, to a positively charged Lysine. This change in charge might affect the interaction between the *nurf-1*-encoded protein and other proteins. However, considering the EVA results and results from DAPI staining, no significant defect in the germline cells was observed in either homozygous hermaphrodites or males, we do not think the single missense mutation has any large impact on meiosis in the absence of the *top-2(it7)* mutation. Also, in the earlier mentioned study of the suppressors that could rescue *top-2*-induced embryonic lethality, the RNAi knockdown of *nurf-1* alone did not rescue embryonic lethality (1.7% progeny) (Bhandari et al., 2020). This suggests that the knockdown of *nurf-1* alone does not suppress the *top-2(it7)* phenotype. Yet whether the single missense mutation E1952K on *nurf-1* can affect the *top-2(it7)* lethality remains unknown. To elucidate if it has any effects on the *top-2*-induced embryonic lethality, CRISPR/Cas9

can be used to induce this single missense mutation *nurf-1* [E1952K] on the *top-2(it7)* line and a following progeny count via embryonic viability assay.

Among the 11 *top-2*-lethality suppressors discovered in Bhandari's study, *mep-1* was discovered as the co-suppressor of *nurf-1*. The knockdown of *mep-1* alone through RNAi was not considered effective in rescuing the *top-2*-induced embryonic lethality since the percent rescued was only 1.0%. However, when it combined with the knockdown of *nurf-1*, the *top-2*-induced embryonic lethality was rescued to a significant percent of 9.2% (Bhandari et al., 2020). This suggests that a potential co-suppressing mechanism may exist. This co-suppressor *mep-1* mutation is identified as a single missense mutation changing the non-charged Glycine (57) to a negatively charged Aspartic acid (Bhandari et al., 2020). In *C. elegans*, *mep-1* encodes a nuclear zinc finger protein (alternative name: MOG interacting and ectopic P-granules protein), which is a part of a chromatin remodeling complex involved in cell fate determination (Unhavaithaya et al. 2002). Interestingly, as depicted in Figure 12(b), the *mep-1* suppressing mutation (G57D) was predicted to happen in a disordered region (0-244), which has not been found to carry any function in the wildtype protein. Whether this single missense mutation can provide some insight to function of the MEP-1 disordered region remains unknown. Also, a series of questions can be asked regarding the co-suppression of *nurf-1* and *mep-1*: how does *mep-1* interact with *nurf-1*? Do they act directly or indirectly? Do they interact with *top-2*? If so, how do they act together? Do they act with the TOP-2 protein in rescuing the *top-2(it7ts)*-induced chromosome-segregation defects? Or do they act together with other proteins to

compensate the missing function from the defected TOP-2 protein? To answer these questions, further analyses will be necessary to elucidate their possible roles in this co-suppression of the *top-2*-induced embryonic lethality.

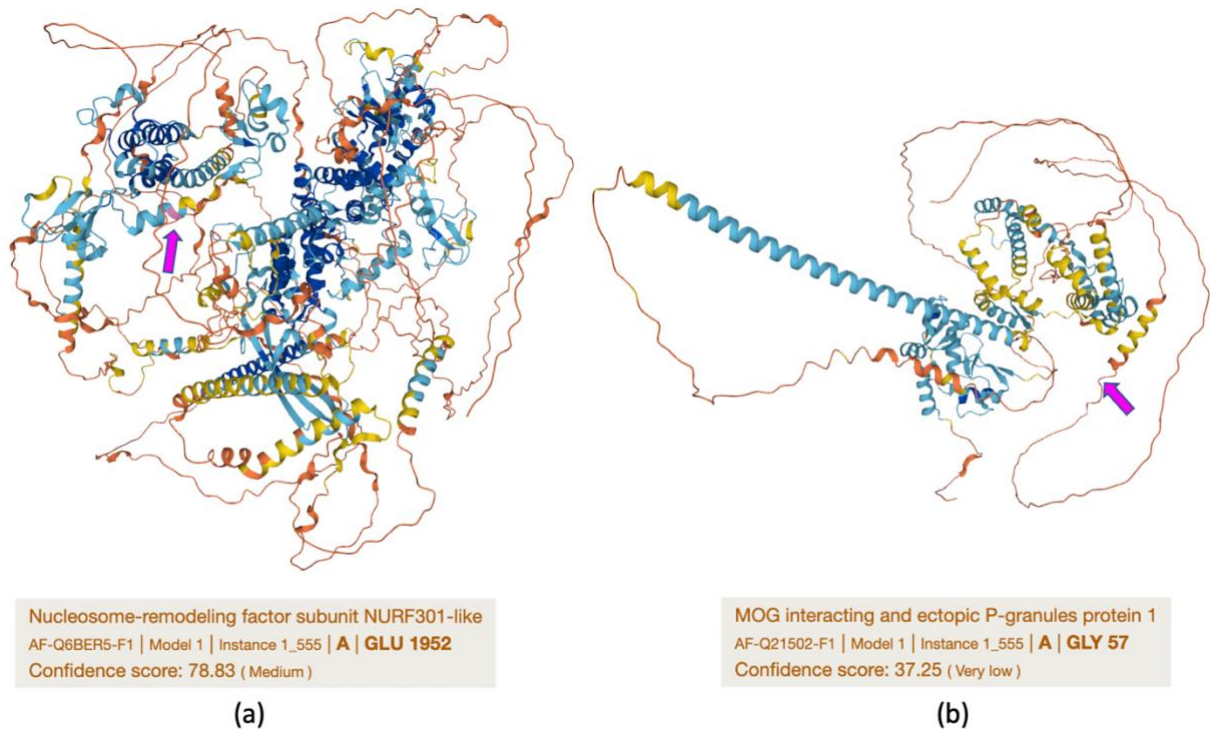


Figure 12. Models of predicative protein structures of the *nurf-1* encoded protein and the *mep-1* encoded protein.

(a) *nurf-1* encoded protein, which is a subunit in the NURF301-like nucleosome-remodeling factor. The CRISPR-induced single missense mutation E1952K is confidently (pLDDT >70) considered to be located on an α helix on a DDT domain (light blue helix marked in light pink and pointed out by a magenta-colored arrow). (b) *mep-1* encoded protein, which is a MOG interacting and ectopic P-granules protein, aka zinc finger protein. The CRISPR-induced single missense mutation G57D is predicted (pLDDT <50) to happen on a disordered region (colored orange; pointed out by a magenta-colored arrow). Both models retrieved and adapted from alphafold. Deep blue color indicates a very high model confidence (pLDDT >90); light blue color indicates a high model confidence (90 > pLDDT > 70); yellow indicates a low model confidence (90 > pLDDT > 70); orange indicates a very low model confidence (pLDDT < 50). pLDDT, per-residue confidence score.

4.2 Further Direction

To further characterize the roles of *nurf-1* and *mep-1* and how they function to suppress the phenotypes of *top-2(it7)*, four new genotypes should be created using CRISPR/Cas9 genome editing: one is the line that contains both single missense mutations of *nurf-1[E1952K]* and *mep-1[G57D]* should be created; and one line that contains all three single missense mutations of *nurf-1[E1952K]*, *mep-1[G57D]*, and *top-2(it7)*; two lines that each contains *nurf-1[E1952K]* and *top-2(it7ts)* or *mep-1[G57D]*, and *top-2(it7)*. The phenotype of each mutant will be observed through whole-mount DAPI stain to reveal any change on the germline cells from the mutations. For the later three lines carrying the combined *top-2(it7)* mutation, the germline cells depicted via whole-mount DAPI stain should be compared to the germline cells from *top-2(it7)*. Additionally, the effects of the double and triple mutants on embryonic viability and fertility/meiosis will be tested in both hermaphrodites and males.

Moreover, structure-function analyses will be conducted to elucidate the protein functions of NURF-1 and MEP-1 as well as the possible mechanism in them acting together as the co-suppressors to the *top-2*-induced embryonic lethality.

Immunofluorescence staining can be performed on both WT protein and the mutant protein to analyze the chromosomal association in each genotype during meiosis. The visualization of WT protein localization can provide information on when and where each protein acts. When compared to the mutant proteins, the changes in the

localization can provide some insight in the possible roles of each protein and how possibly they interact with each other.

Chapter 5

CONCLUSION

In summary, *nurf-1* gene was characterized in this study via analyzing its mutant genotype with 725bp deletion (*n4293Δ*) as well as its CRISPR-induced genotype with a single missense mutation (*ude34*)[*E1952K*]. Though the deletion was confirmed to have an effect in germline cell proliferation in causing sterility in hermaphrodites, no evidence showed that the single missense mutation has caused any defects in either the hermaphrodite or the male germline cells. This result matched the data from the earlier study that the single missense mutation *nurf-1*(*ude34*[*E1952K*]) alone does not rescue the *top-2*-induced embryonic lethality [1.7% (Bhandari et al., 2020)]. However, when RNAi knockdown of *nurf-1* and *mep-1* was induced at the same time, the progeny rescued percent has significantly raised to 9.2% (Bhandari et al., 2020). This indicates a possible co-suppression mechanism exist from the interaction between *nurf-1* and *mep-1*. Further characterization is necessary in the genotype carrying the combination of the two single missense mutations. In addition, structure-function analyses will be needed to elucidate the roles of both *nurf-1* and *mep-1* in spermatogenesis/oogenesis as well as their possible interactions with *top-2*.

REFERENCES

- Alkhatib SG, Landry JW. The nucleosome remodeling factor. *FEBS Lett.* 2011 Oct 20;585(20):3197-207. doi: 10.1016/j.febslet.2011.09.003. Epub 2011 Sep 9. PMID: 21920360; PMCID: PMC4839296.
- Andersen, E. C., Lu, X., & Horvitz, H. R. (2006). *C. elegans* ISWI and NURF301 antagonize an Rb-like pathway in the determination of multiple cell fates. *Development (Cambridge, England)*, 133(14), 2695–2704. <https://doi.org/10.1242/dev.02444>
- Anderson, J. L., Morran, L. T., & Phillips, P. C. (2010). Outcrossing and the maintenance of males within *C. elegans* populations. *The Journal of heredity*, 101 Suppl 1(Suppl 1), S62–S74. <https://doi.org/10.1093/jhered/esq003>
- Bhandari, Nirajan., Rourke, Christine., Wilmoth, Thomas., Bheemreddy, Alekya., Schulman, David., Collins, Dina., Smith, Harold E., Golden, Andy., and Jaramillo-Lambert, Aimee., G3: GENES, GENOMES, GENETICS *April 1, 2020 vol. 10 no. 4 1183-1191*; <https://doi.org/10.1534/g3.119.400927>
- Barak, O., Lazzaro, M. A., Lane, W. S., Speicher, D. W., Picketts, D. J., & Shiekhattar, R. (2003). Isolation of human NURF: a regulator of Engrailed gene expression. *The EMBO journal*, 22(22), 6089–6100. <https://doi.org/10.1093/emboj/cdg582>
- Brent Cornell. BioNinja. (n.d.). Retrieved May 4, 2022, from <https://ib.bioninja.com.au/higher-level/topic-10-genetics-and-evolu/101-meiosis/stages-of-prophase.html>
- Corsi AK, Wightman B, Chalfie M. A Transparent Window into Biology: A Primer on *Caenorhabditis elegans*. *Genetics*. 2015 Jun;200(2):387-407. doi: 10.1534/genetics.115.176099.
- Deweese, J. E., & Osheroff, N. (2009). The DNA cleavage reaction of topoisomerase II: wolf in sheep's clothing. *Nucleic acids research*, 37(3), 738–748. <https://doi.org/10.1093/nar/gkn937>
- Hamiche, A., Sandaltzopoulos, R., Gdula, D. A., & Wu, C. (1999). ATP-Dependent Histone Octamer Sliding Mediated by the Chromatin Remodeling Complex NURF. *Cell*, 97(7), 833–842. doi:10.1016/s0092-8674(00)80796-5
- Hillers, Kenneth. (2015). Meiosis. *WormBook*. 2017. 1-54. 10.1895/wormbook.1.178.1.
- Huang, C., Xiong, C., & Kornfeld, K. (2004, May 25). *Measurements of age-related changes of physiological processes that predict lifespan of Caenorhabditis elegans*. Retrieved January 25, 2021, from <https://www.ncbi.nlm.nih.gov/pmc/articles/PMC419561/>
- Jaramillo-Lambert, A., Fabritius, A. S., Hansen, T. J., Smith, H. E., & Golden, A. (2016, December). The Identification of a Novel Mutant Allele of topoisomerase II in

Caenorhabditis elegans Reveals a Unique Role in Chromosome Segregation During Spermatogenesis. Retrieved from <https://www.ncbi.nlm.nih.gov/pubmed/27707787>

Large, E. E., Xu, W., Zhao, Y., Brady, S. C., Long, L., Butcher, R. A., Andersen, E. C., & McGrath, P. T. (2016). Selection on a Subunit of the NURF Chromatin Remodeler Modifies Life History Traits in a Domesticated Strain of *Caenorhabditis elegans*. *PLoS genetics*, *12*(7), e1006219.
<https://doi.org/10.1371/journal.pgen.1006219>

Libretexts. (2022, April 9). *11.1: The process of meiosis*. Biology LibreTexts. Retrieved May 4, 2022, from [https://bio.libretexts.org/Bookshelves/Introductory_and_General_Biology/Book%3A_General_Biology_\(OpenStax\)/3%3A_Genetics/11%3A_Meiosis_and_Sexual_Reproduction/11.1%3A_The_Process_of_Meiosis](https://bio.libretexts.org/Bookshelves/Introductory_and_General_Biology/Book%3A_General_Biology_(OpenStax)/3%3A_Genetics/11%3A_Meiosis_and_Sexual_Reproduction/11.1%3A_The_Process_of_Meiosis)

Nitiss, J. DNA topoisomerase II and its growing repertoire of biological functions. *Nat Rev Cancer* **9**, 327–337 (2009). <https://doi.org/10.1038/nrc2608>

Suehyb G. Alkhatib, Joseph W. Landry, The Nucleosome Remodeling Factor, FEBS Letters, Volume 585, Issue 20, 2011, Pages 3197-3207, ISSN 0014-5793,
<https://doi.org/10.1016/j.febslet.2011.09.003>.

Wysocka, J., Swigut, T., Xiao, H. *et al.* A PHD finger of NURF couples histone H3 lysine 4 trimethylation with chromatin remodelling. *Nature* **442**, 86–90 (2006).
<https://doi.org/10.1038/nature04815>

Yin, D., & Haag, E. S. (2019, June 12). *Evolution of sex ratio through gene loss* / *PNAS*. Vol. 116, No.26. Retrieved March 13, 2022, from <https://www.pnas.org/doi/10.1073/pnas.1903925116>